Chapter 6

6.1 Introduction

Dextrins are linear *a*-(1,4)-linked D glucose polymers obtained by enzymatic hydrolysis of corn starch. They also contain (<5%) 1,6 links thus show branching as well. However dextrin and starch has same molecular formula $[C_x(H2O)_y)]^{n-}$ (y = x - 1) where glucose units are linked to each other, dextrin is short, small and less complex molecule than starch.[213] Dextrin are most promising candidates commonly used in the manufacturing of adhesives for envelopes gum tapes postage stamps and water labelling due to its low viscosity and solution stability at higher temperature. Diversification of dextrin by grafting or crosslinking is a significant approach that derives the benefit of combining a natural polysaccharide and a synthetic polymer for different bio medical applications including protein delivery [214] MRI agent, superabsorbent materials,[215] as a cross linker [216], drug delivery[217]. By grafting synthetic polymers on natural polymers backbone is an outstanding way to develop polymers with improved functional properties and a suitable drug carrier as well. Thus the composition and structure of the polymers play a significant role in tuning the release rate of drug.[218] Chemical grafting is one of the most effective methods for modifying structure and properties of natural polymers. Graft copolymerization of natural polysaccharides is becoming an important resource for developing advanced materials as it can improve the functional properties of natural polysaccharides.[219]. In this sense, a new generation of grafted copolymers combining-starch derivatives and methyl methacrylate (MMA) polymers has been introduced as direct compression excipients. These materials form, under compression, inert matrices able to

control the release of the model drug (anhydrous theophylline) by a diffusion mechanism through the matrix porous structure [220]. Polyurethanes belong to special class of synthetic polymers owing to biodegradable and biocompatible nature and currently used in drug delivery applications.[221-223] and shape memory properties [127, 171]. These are highly versatile polymers with varying molecular designs that can be easily tuned by altering either hard or soft segment i.e di-isocynate, diol and chain extender accordingly. Other than traditional applications of PUs investigations on development of biodegradable PUs for biomedical applications like temporary scaffold, control release of active ingredients[224] and ligament reconstruction prosthesis. Hydrophilic PEO based PU hydro gels have been synthesised and presented desired characteristics of polyurethanes and can be used for drug delivery applications[225]. Grafting of polyurethanes on dextrin can be a new frontier for developing biodegradable and biocompatible polymers, utilizing them as drug delivery carrier. Our interest lies in investigation of novel chemically connected, biocompatible graft copolymer for sustained dug delivery application.

Here in this article we have designed and prepared polyurethane grafted dextrin graft copolymer and investigating the feasibility of these copolymers as a new drug carrier for controlled delivery of anti-cancerous dexamethasone which is used in the present article. Synthesised copolymers were characterised via various spectroscopic techniques and grafting was confirmed by ^{1}H NMR and GPC. Interactions among the polymer chains were visualised by FTIR and NMR providing evidence of chemical reaction between dextrin and polyurethane. Thermal degradation behaviour and their melting temperatures were determined and mechanical analysis of copolymers was also done for understanding the stability of these systems. Grafting PU on dextrin resulted in enhanced thermal and

mechanical stability thereby making them stable than dextrin. Drug release study elucidated the advantage of grafting showing a sustained and slow release of drug when compared to pure dextrin. Further the assessment of biocompatibility of grafted systems were done by MTT assay using Human cervical cells (Hela), the developed copolymers were nontoxic and exhibited good biocompatibility. The *in vitro* and *invivo* drug release using dexamethasone has been evaluated for anti tumour activity. Thus sustained release and enhanced biological activities made these grafted systems a better drug carrier thereby reducing the other adverse effects of drug. To best of our knowledge no such other reports are available where grafting of PU on dextrin has been done for a better drug delivery vehicle.

6.2 Results and discussion

6.2.1 Spectroscopic evidence of grafting

Different copolymers through grafting of PU onto dextrin with varying graft density having different chemical properties were synthesized. The general scheme of chemical reaction between PU and dextrin is presented in ***scheme 2.4*** presented in experimental section where hydrophilicity of dextrin is altered by extent of grafting of PU thereby maintaining hydrophilic and hydrophobic balance. Grafting of PU chains on linear dextrin backbone occurs via chemical reaction between isocaynate terminated prepolymer and hydroxyl groups of dextrin forming urethane linkages (-NHCOO-) with various graft density of PU, therefore the developed graft were identified as brush polymers with dense and sparse distribution of PU chains. Grafting was confirmed via ^{1}H NMR spectroscopic technique and graft density i.e degree of substitution is calculated by integrated peak area under the peaks [226]. Typical representative NMR spectra of pure dextrin, PU and its brush

polymers is presented in ***Figure 6.1a***. Since dextrin contains three hydroxyl groups two secondary and one primary and among them the reactivity of primary is highest thus the chemical reaction of PU is assumed to occur with C6 OH forming urethane linkage. The appearance of new signal at 7.0 ppm labelled as '***a'*** in the spectrum is due to urethane proton (-NHCOO-), formed through reaction of isocynate of PU with hydroxyl of dextrin. The degree of substitution was calculated from integrated peak area of the peaks of CH of PTMG and primary OH of dextrin.

The DS % was found to be highest for D-P-H 30% and 15% for D-P-L using long chain PU as grafts and the polymers are named accordingly where D is dextrin, P is the PU prepolymer and H and L signifies the high and low graft density of PU. The typical NMR spectra of dextrin in DMSO-d6, 400 MHz, showed peaks between δ=4.46 and 4.67, which are attributed to protons at position 2, 3, 4, 5 and 6 (H^2-H^6). The absorbance peaks between δ=4.86 and 5.15ppmare due to anomeric proton (H^1). Beside the peaks situated at δ=5.32 and 5.6 represents OH-2 and OH-3 which are clearly separated from primary hydroxyl group centered on 4.2-4.5 ppm presented in ***Figure 6.1a*** [227]. The chemical reaction of PU with dextrin is interpreted from the appearance of peak at δ~4 ppm due to proton of HMDI in the grafted polyurethane chains along with another new intense peak at δ~1.5 ppm, assigned to methylene proton of PTMG presented in *inset* ***Figure 6.1a***, while the peak of urethane proton from PU is centered at 8 ppm. The presence of peak at δ= 7 ppm in different brush copolymers and its absence in PU ensures the incorporation of PU onto dextrin backbone. Here it is important to mention that formation of graft against physical mixture of dextrin and P is ruled out, since in NMR spectra of physical mixture absence of peak at 7 ppm which is direct evidence of grafting is absent ***(Figure 6.1a).*** Therefore NMR

provides direct evidence of grafting PU on dextrin backbone. The solid state NMR of pure dextrin (D), PU(P) and its graft is demonstrated in ***Figure 6.1b,*** the NMR spectra of dextrin and prepolymer revealed all the characteristic peaks as per literature, in graft peaks due to urethane carbonyl carbon were located at 157 ppm which further verifies grafting of PU on dextrin.

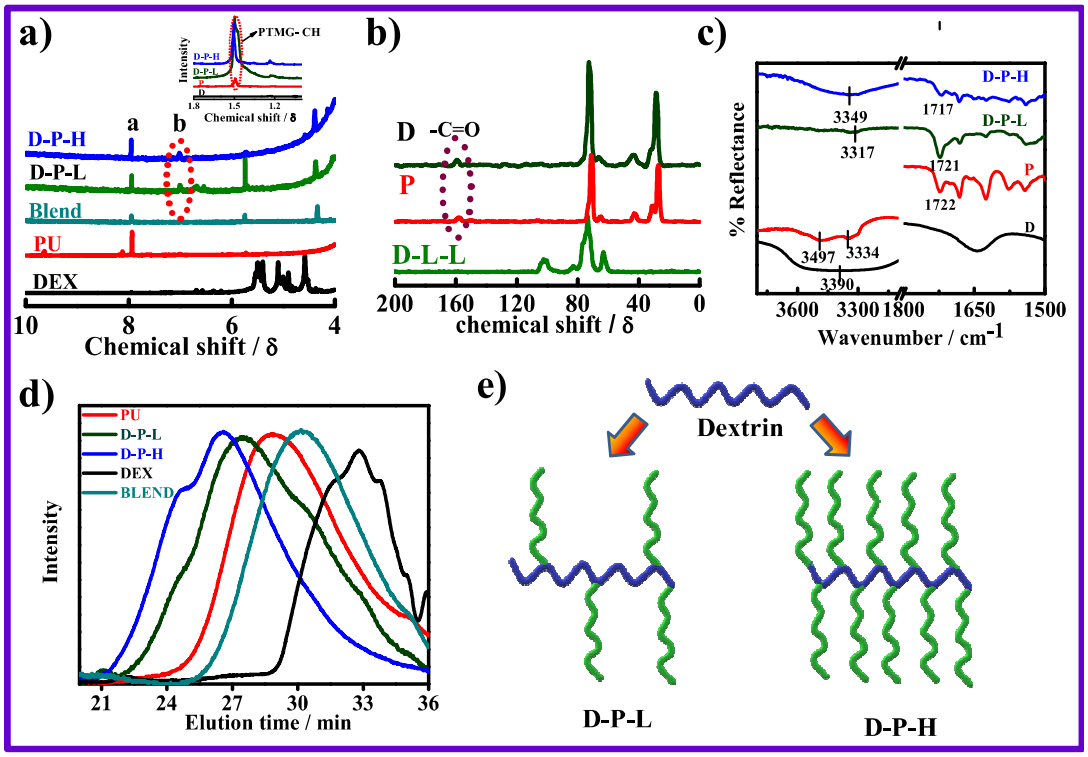

Figure 6.1: *a) ^{1}H NMR Spectra of Dex, PU and their indicated grafts showing new peak position due to grafting marked by 'b' and change of hydrogen bonding as presented marked by 'a'. b) ^{13}C NMR Spectra of Dex, PU and their indicated grafts* ***c)*** *FTIR spectra of pure Dex, PU and their graft copolymers as indicated; d) Gel permeation chromatogram of graft copolymers showing lower elution time for high graft density copolymers; and e) Schematic presentation of the architecture of all the graft copolymers with varying graft density.*

Verification of grafting/chemical tagging of PU is further shown through FTIR spectra showing characteristic peaks at 1720 cm^{-1} assigned for urethane >C=O band and 1546 cm^{-1}

due to NH bending respectively[228] (***Figure 6.1c)***. A strong hydrogen bonded carbonyl peak was observed in PU and its intensity decreases with decrease in graft density signifying that insufficient intermolecular hydrogen bonding in sparsely grafted brush polymers. A little shifting in free carbonyl peak in all copolymers is observed which is probably due to interaction with neighboring polar NH groups. In pure dextrin broad peaks lying in the region 3000-3600 cm^{-1} principally due to multiple hydroxyl groups become narrower as well as shifted to lower wave number on grafting[229]. The peak in this region for PU splits into two peaks at 3497 and 3334 cm^{-1} for free and hydrogen bonded >N-H stretching, respectively, while this peak is shifted to 3325 and 3342 cm^{-1}in D-P-L and D-P-H respectively indicating intermolecular hydrogen bonding persist in both the brushes. Altering the PU graft density increases the molecular weight of polymer which was measured through gel permeation chromatography. Synthesized brush polymers showed high molecular weight as compared to P with low elution time and low refractive index. Highly graft brushes D-P-H exhibited higher molecular weight while sparsely graft brushes D-P-L displayed low molecular weight (***Figure 6.1d)*** and were, 83k and 23k, respectively, with relatively low polydispersity index of ~1.35. In case of densely grafted brush a bimodal distribution is seen revealing the presence of two molecular species arising due to slight cross-linking in addition to normal highly graft brush. Molecular weight of physical mixture was almost similar to PU further supporting grafting of PU onto dextrin (***Figure 6.1d)***.

Nevertheless it's clear that through grafting molecular weight of brushes increases as expected. It is relevant that high and low graft density would generate different architectures of brushes as represented in form of cartoon in ***Figure 6.1e*** measured from

graft density calculation through NMR and followed by molecular weight matching as well. The designed wide range of brushes with different interacting behaviour is most suitable as a biomaterial, carrier for biologically active agents by changing hydrophilic and hydrophobic balance.

6.2.2 Thermal and mechanical responses with structural alteration in brush copolymer

Thermal behaviour of pure dextrin and its brush polymers was known through TGA and DSC analysis. Thermogram of pure dextrin revealed two stage weight loss, the initial weight loss corresponds to the traces of moisture in the sample lying in the region between 80-130 ^{o}C, while the second zone at 230-350 ^{o}C is due to complete degradation of polysaccharide back bone including secondary as well as primary alcohol group (CHOH and CH_2OH), while in case of brushes thermal stability was enhanced by 60-70 ^{o}C after grafting with PU chains as shown in (***Figure 6.2a)***. Degradation temperatures for D-P-H and D-P-L are found to be 345 and 350 ^{o}C respectively, showing higher thermal stability of brushes as compared to native dextrin. Degradation of PU occurred at higher temperature at 374 ^{o}C and due to attachment of this PU chain on dextrin moiety enhances the thermal stability of brush copolymers. Here it is important to mention that temperature at 5 % weight loss is considered at degradation temperature. Further from DSC analysis PU shows single endothermic peak at 38 ^{o}C due to melting of soft segment content while in case of brush polymers two endotherms were observed in the range of 25-40 ^{o}C (***Figure 6.2b)***. A small endothermic peak at higher temperature at 112 and 116 ^{o}C for D-P-L and D-P-H is due to hard segment content in copolymers. As graft density of PU increases, more hard segment crystallisation occurs causing the hard segment melting peak towards higher temperature.

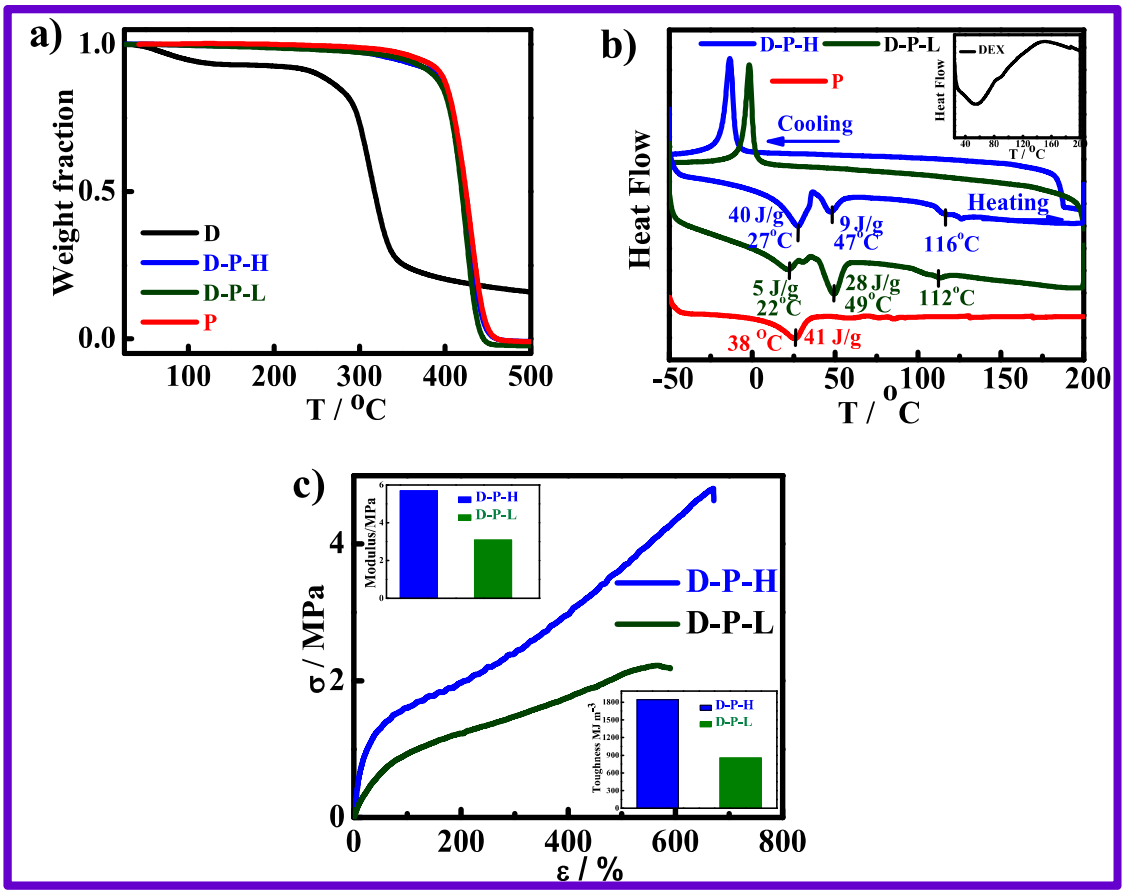

Figure 6.2: *a) Thermal stability (TGA thermogrammes) of pure Dextrin, prepolymer (P) and their grafts D-P-L and D-P-H as measured through thermogravimetric analyzer; b) DSC thermogrammes of P D-P-L and D-P-H as indicated both for heating and cooling cycle (top two thermogrammes). Melting temperature and heat of fusions are mentioned in corresponding colour code. The inset figure represents DSC pattern of pristine Dextrin; c) Stress–strain curves of D-P-L and D-P-H. Inset bar graphs indicate the modulus and toughness of the copolymers.*

In addition to shifting in melting temperature for graft copolymers the reduction in heat of fusion values calculated from area under the endothermic peak to 27 and 39 Jg^{-1} for D-P-L and D-P-H when compared to pure PU 41 Jg^{-1} indicates interaction between P and dextrin chains. However relatively more reduction of δH in D-P-L indicates higher interaction vis-à-vis D-P-H also supported by other spectroscopic techniques. Moreover, delayed

crystallization in D-P-H over D-P-L during cooling also suggests relatively stronger interactive system in high graft density copolymer than that of low density graft copolymer (two above thermogrammes in ***Figure 6.2b***. However, better thermal stability and stronger interaction is evident from the thermal measurements.

Mechanical testing was done for understanding the strength and toughness of graft copolymers. Importantly the elongation at break for densely graft brush polymer was substantially increased with increasing degree of substitution in D-P-H due to slight amorphous nature while in case of sparsely graft brush polymer was considerably stiffer which arises from its higher crystalline nature (***Figure 6.2c)***. The coherency of hard segment and predominant intermolecular hydrogen bonding between PU chains is responsible for higher elongation in break for densely grafted long chain brush polymer. Hence the toughness values calculated from area under stress strain curve are 1840 MJ m^{-3} for D-P-H and 850 MJ m^{-3} for D-P-L respectively, a clear evidence for toughness of brush copolymers with high graft density. This enhanced mechanical properties due to existence of multiple hydrogen bonds between urethane linkages (discussed from FTIR section) with adjacent PU linkages, during motion of PU chains deformation may cause pulling of brush polymer which is connected to other dextrin moiety through PU chain there by providing an additional energy dissipation mechanism. During this dragging of one dextrin molecule from other through covalently grafted PU chains most of the load was transferred through the H bonds causing disruption which leads to maintain structural flexibility of PU [230]. Elastic modulus/stiffness calculated from the initial linear slope was again higher for highly grafted brush polymer and was as compared to low density graft because of their crystalline difference which is substantiated from DSC section where slight amorphous behaviour is

present against highly crystalline peaks for D-P-L. Thus stiffness, toughness and modulus can be easily tuned just by varying the graft density of PU. Pure PU and Dex were highly crystalline and their films could not be prepared thus there mechanical testing could not be done using UTM.

6.2.3 Structural and surface characterization

For better understanding the grafting, with varying graft density of PU on dextrin small angle neutron scattering of brush copolymer are performed clearly showing a shoulder at wave vector, q ~ 0.25-0.30 nm^{-1}, corresponding to the characteristic length Λ_c 22.1, 22.1, 22.4, 20.25 for D, P, D-P-L and D-P-H respectively, indicating that lesser number of molecules are required for highly grafted system to form self assembly (***Figure 6.3a)***. The correlation length ξ as calculated from Debye-Buche fitting of initial wave vector are found to be 1.5, 1, 1 and 0.5 nm for D, P, D-P-L and D-P-H, respectively, clearly demonstrate the smaller blob size in highly graft brush polymers than that of pure PU. Polyurethanes is very prone to form aggregate through hydrogen bonding between hard and soft segment of chains and the blob size generally increases in presence of nano fillers in PU, while in case of grafting of PU on to linear dextrin chain give rise to different blobs through inter and intermolecular hydrogen bond among grafted P chains hence number of blobs increases and their individual size decreases in D-P-L and D-P-H gradually with increasing graft density. These crystallites assemble in lager self assembled domains due to hydrogen bonds observed in AFM section. The size of inhomogenities in dextrin is 1.5 nm and this bigger size is due to extensive hydrogen bonding amongst dextrin molecule due to multiple OH present resulting in larger blob size. Nevertheless SANS data satisfactorily supports the various designed brush polymers and their subsequent agglomeration. In short, mechanical

and thermal properties can be tuned by varying the graft density and graft length in brush copolymers thereby make them suitable for drug delivery vehicle with proper thermal and mechanical stability based on their unique structure. AFM imaging is well suited to visualize the surface topography of polymeric films along with the roughness and average size of the inhomogeneties. Granular Pure dextrin had particle size morphology, oval shaped molecules. Particles of pure dextrin are observed with the average dimension of 300 nm (***Figure 6.3c***). Strip like morphology is evident in D-P-H whose intensity has significantly enhanced due to hydrogen bonded agglomeration in the hard segmented zone as discussed earlier. While stronger strip morphology was observed in P arising from assemblage of hydrogen bonded hard segment as reported earlier. Due to extensive intermolecular hydrogen bonding in hard segment domain in D-P-H self assembly occurs. AFM images shows a distinct phase separation between dark phase (softer matrix) regions surrounded by light coloured i.e. hard segment especially in highly graft brush polymers [140]. The incorporation of PU on to dextrin leads to change in microstructures of synthesized polymers. In D-P-H due to more grafting of PU the hard domains forms self assembly due to inter molecular hydrogen bonding arising from inter chain interactions among C=O and N-H groups causing change in morphology. Greater inhomogenities present is further evident from optical images (***Figure 6.3d)*** and larger dimensions of agglomerates are noticed in D-P-H (5 μm) as compared to D-P-L (2.5 μm). Here in this event self assembly in brush copolymers is evident from the nano meter dimensions of blob size obtained from SANS, assembled to form 100 nm strip size observed in AFM, which further accumulated micro clusters of 2-5 μm measured from optical images and this systematic self assembly from nm dimensions very smaller size to μm size is

predominantly through hydrogen bonding. Such a bottom up approach in the construction of self assembly is most suitable for biologically active molecules to bind and can be released in more sustained way.

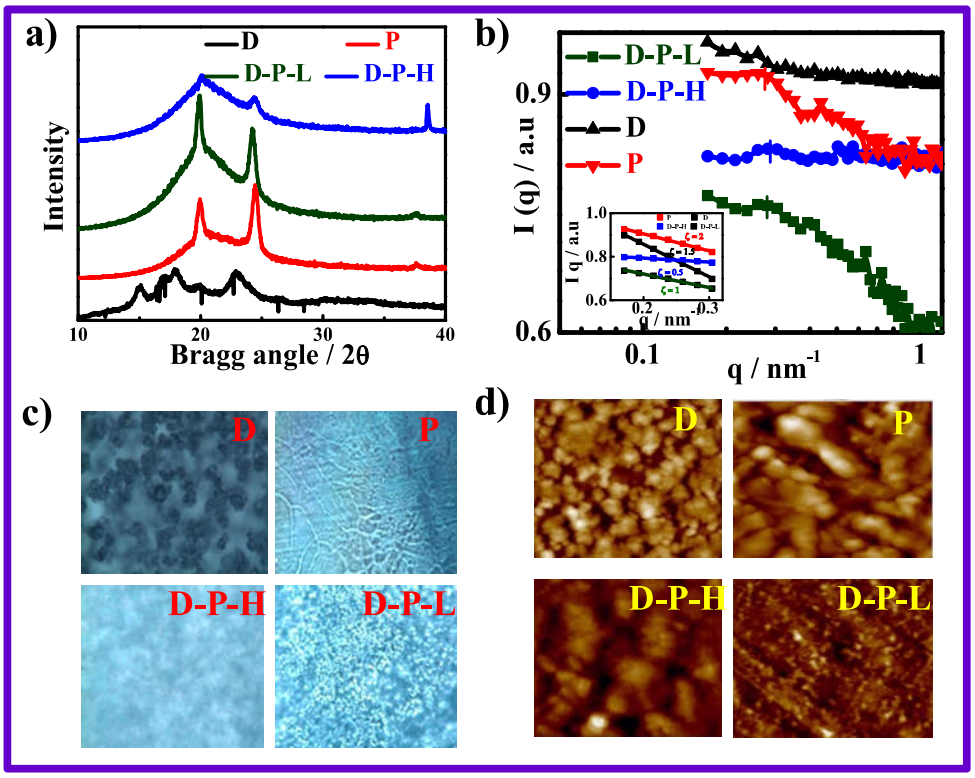

Figure 6.3: *Structural and morphology investigation, a) XRD patterns of pure Dextrin, PU and their graft copolymers; b) Small angle neutron scattering profile of D and P and its graft copolymers. Inset figures represent the Debye-Bueche fitting of the initial data points showing the correlation length; c) Optical images of the graft copolymers showing greater agglomerates. d) AFM images of Dextrin, P and their grafts in semi contact mode (10×10 μm^2).*

6.3 *In Vitro* drug release from brush polymers/hydrogel

In earlier section discussed above we found that developed brush copolymers were mechanically strong, thermally stable, and self assembly made them suitable material especially for *in vitro* drug release. Sustained drug release is of prime concern to regulate

the concentration of drug in blood stream for longer time and to obtain higher efficacy of drug without causing any side effects. 5 wt % of drug w.r.t pure polymer was embedded in various designed brush polymers through solution route and drug loaded polymeric films were obtained, their in-vitro release study was done at pH 7.4 in PBS solution at 37 ^{o}C. Release behaviour of model drug dexamethasone from the brush co polymers as well as from dextrin as a function of time is shown in ***Figure 6.4***, the release profiles drug loaded dextrin followed burst release and almost 100% release within 2 h was observed, this is probably due to dissolution and diffusion of poorly entrapped drug into dextrin, while in case of brush copolymers striking sustained release pattern was obtained. Dramatically low graft density brush D-P-L showed more sustained release pattern vis-à-vis high graft density brush (D-P-H). As discussed in previous sections in D-P-L there occurs intra molecular hydrogen bonding between PU chains with dextrin moiety predominantly against intermolecular hydrogen bonding in densely grafted brush polymer leading to open structure while in less graft wrapping of PU chains leads to squeezed structure which entraps the drug in better way resulting in sustained release pattern. Based on these designs of brush polymers a schematic diagram is presented (***Figure 6.4b).*** Nevertheless burst release in dextrin was overcome by grafting PU chains and sustained release of 73 &63 % was observed for D-P-H and D-P-L respectively during 40 h. Since the release of drug from D-P-L follows ideal pattern means there is always some of drug getting released with time, thus we prepared hydrogel of this system. Here, methyl cellulose gel (MC gel) is used and D-P-L is embedded in MC gel and is termed as D-P-L-MC. Drug loaded D-P-L is incorporated in MC gel (through solution route) following the schematic shown in ***Figure 6.4b*** and is termed as '*D-P-L-MC-D*'. Release of drug from D-P-L-MC-D was further

sustained and almost 65 % release was observed in similar time frame. The advantage of incorporating this system in MC gel is that the system becomes injectable gel and can be injected subcutaneously at the tumor site for targeted release by constant drug diffusion. Release of drug through polymer matrix depends on various factors such as penetration of solvent into the matrix, dissolution of the drug and finally, the diffusion of drug from the matrix polymer. Amongst these steps any of these can be rate determining for drug release kinetics. Delayed diffusion of drug in brush copolymers was observed as compared to pure dextrin. For understanding the drug release mechanism, different kinetic model have been used to fit the release pattern from designed brush polymers. The release kinetics is well fitted with korsmeyer peppas model having higher linear correlation coefficient values with r^2 -0.98 and having the exponent values as indicating non Fickian diffusion for ($n \geq 0.45$) diffusion kinetics of drug molecules through all the systems except for D-P-L **[141].** Other kinetics model such as zero order, first order and Higuchi models are presented in ***Figure 6.5*** *and* ***table 6.1.*** Slow diffusion of drug is due to covering of hydrophobic PU chains on to hydrophilic dextrin backbone thereby maintaining hydrophilic and hydrophobic balance. Sustained release of drug through polymer matrix is mainly governed by diffusion process where drug diffuses out the tangled path created by grafted polymeric chains. Extent of hydrophobicity was examined through contact angle measurement of polymeric films and the higher value 140 ^{O} for less graft brush polymer against lower value 75 for densely graft brush suggest the hydrophobic nature of D-P-L which further coalesced the cartoon structure just by controlling the graft density of PU which regulates the drug release profile from drug loaded polymer films. The hydrophobic component in polymer matrix disrupts the packing of polymer chain causing pore formation and this leads to faster release of

drugs. Open structure of D-P-H revealed from SANS data showed more swelling behaviour less hydrophobicity as compared to D-P-L prominently due to more water absorption through hydrogen bonding a clear evident for hydrophilic nature of D-P-H.

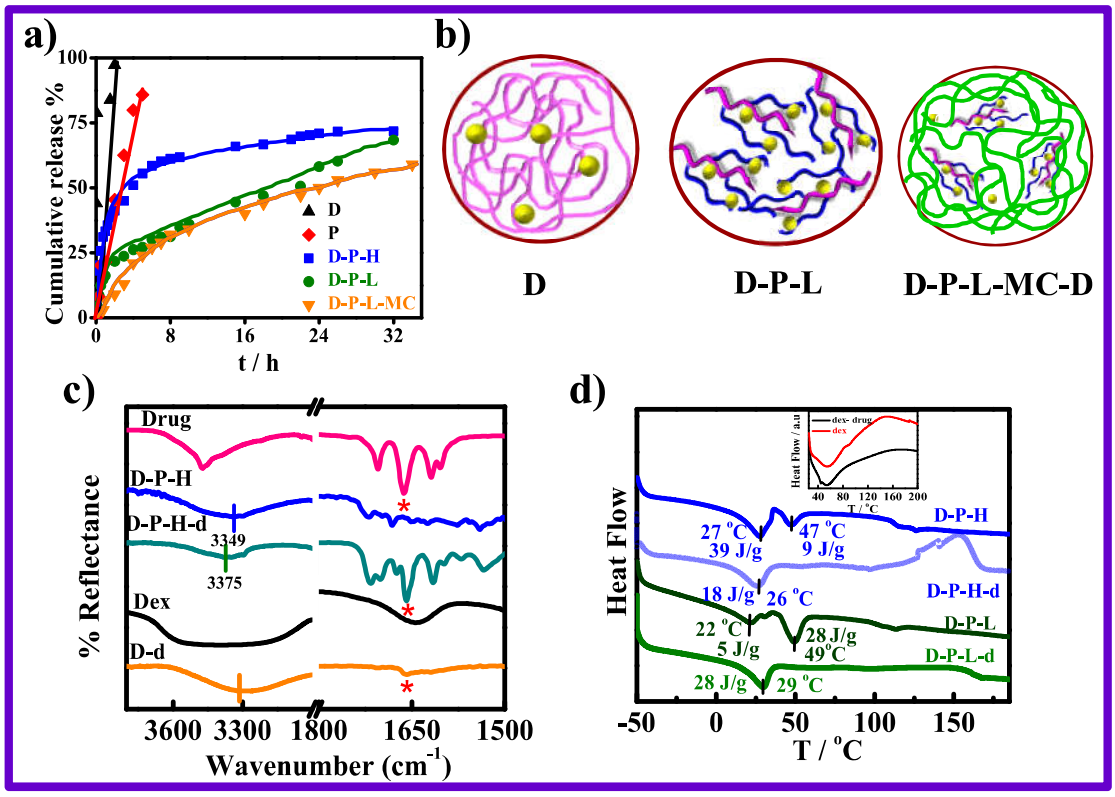

Figure 6.4: *a) Cumulative release profiles of drug loaded graft copolymers and injectable gel indicated, showing controlled drug release profile from graft copolymers and gel; b) Schematic model showing the drug release from graft copolymer and gel. c) FTIR spectra of pure and drug loaded systems, shifting in peaks indicating interactions d) DSC thermogrammes of pure and drug loaded systems indicating lowering in melting peak along with reduced heat of fusion values.*

Here the interactions between drug and polymers which are only responsible for the sustained release of drug are evaluated using spectroscopic and thermal techniques like FTIR, and DSC studies. From FTIR spectra of pure drug and drug loaded polymer in

Figure 6.4 c the characteristic peaks in pure drug appeared at 873 and 1666 for CH bending and Carbonyl group, presence of these peaks in copolymers illustrates the successful incorporation of drug in the copolymer. More over the shifting of peaks in drug loaded copolymers was observed indicating interactions are basically dipole dipole and hydrogen bonding. The DSC thermogrammes of representative pure copolymer and drug loaded copolymers (D-P-H-d) are presented in ***Figure 6.4d***. Reduction in the melting temperature of the drug loaded graft copolymers to 27 ^{o}C compared to pure copolymer melting of 47 ^{o}C indicates the interaction between the polymer and drug component and the reduction of ~10^{o} suggest strong interaction between the components. Similar trends were observed for drug loaded D-P-H system. More over the significant lowering of heat of fusion again supports the greater interaction between polymer and drug.

Table 6.1: *Release constant k, correlation coefficient (r), release exponent (n) calculated from various models for drug loaded dextrin and its respective copolymers.*

Sample	First order		Zero order		Higuchi		Korsmeyer Peppas	
	k	r^2	k	r^2	k	r^2	n	r^2
D	0.12	0.33	21.8	0.36	48.7	0.53	0.14	0.53
PU	0.23	0.83	19.35	0.98	40.5	0.93	0.77	0.97
D-P-H	0.1	0.78	9.87	0.74	23.7	0.94	0.33	0.99
D-P-L	0.15	0.59	5.73	0.78	13.5	0.95	0.52	0.93
D-P-L-GEL	0.12	0.75	6.12	0.80	15.4	0.94	0.43	0.98

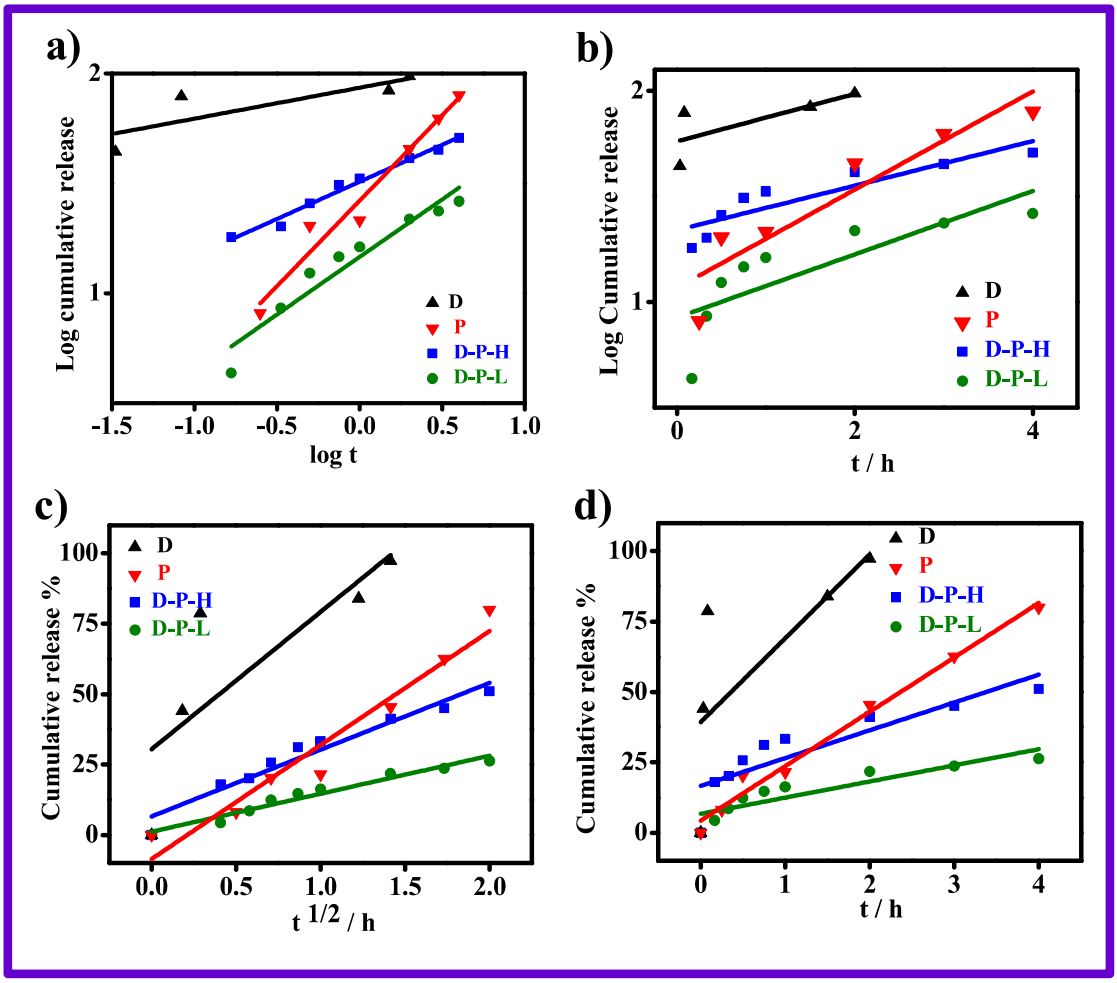

Figure 6.5: *Mathematical models for drug release kinetics a) Korsmeyer- Peppas model, b) First order model, c) Higuchi model d) Zero order model.*

6.4 Biocompatibility studies

For a good drug delivery vehicle, biocompatibility of the material is an essential requirement for its biomedical use and it can be analyzed in vitro through cell viability of the cells over its surface. Viability of Hela cells over pure dextrin and its brush copolymers was evaluated using MTT assay at different interval of time. MTT assay depends on Cellular metabolic activity of NADPH enzyme which reduces MTT reagent to purple colour formazon crystals in viable cells. Cell viability for graft copolymers increases with

time as compared to pure dextrin and an overall increase in viability for all the grafted systems was observed illustrating biocompatible and non toxic nature of nascent grafted copolymers towards cancerous cells for drug delivery applications. (***Figure 6.6a)*** shows cell viability after 24 h of incubation for pure dextrin and its respective brush polymeric films. Cells displayed higher proliferation rate in pure dextrin and grafted systems, this higher cell density signifies the higher cell viability confirming the non toxicity of brush copolymers. However relatively cell viability was higher for densely grafted systems when compared to less grafted one in similar time frame indicating its better biocompatible behaviour vis-a-vis pure dextrin. Fluorescence images of the cells after incubation of 24 h is shown in (***Figure 6.6b),*** cells are well spread and adhered very well on polymeric films further confirming the bio compatibility of these polymeric systems. The higher number density of cells grown on brush copolymers and better proliferation rate further confirms their superior biocompatibility nature.

Cell adhesion studies have also been performed by using Hela cells ensuring biocompatibility and also for bio medical application of materials. Grafted polymers exhibited higher optical density when compared to control resulting in better biocompatibility vis-à-vis pure polymer **(*Figure 6.6c)***. Better cell proliferation of brush copolymers (***Figure 6.6d)*** also supports the optical density data. Thus, the synthesized brush copolymers possess fantabulous biocompatibility, and cells can grow very well on the surface of these brush polymers. Thereby, these are the most effective drug carriers in real applications. Now, the efficacy of sustained drug release from these brush copolymers could be further explored by cell killing with respect to pure dextrin.

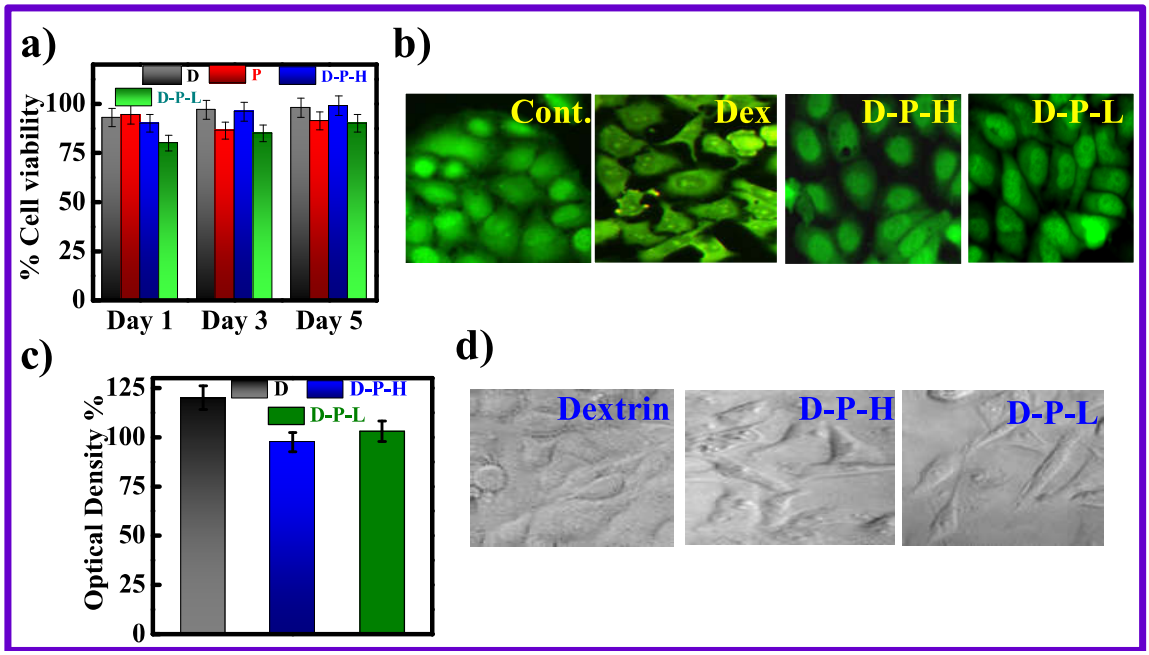

Figure 6.6: *Biological responses of brush polymers through cellular studies. a) Cell viability of indicated samples at time interval of 1, 3 and 5 days through MTT assay measurement; b) Fluorescence microscopic images of cell cultured on indicated specimens and images are taken after one day of cell proliferation (mag 40×); c) Quantification of cell adhesion through optical density measurement of adhered cells over various sample surface; d)Morphology of cells grown on different sample surface as indicated (cell adhesion).*

6.5 Cellular uptake and Cytotoxicity studies

It is customary that the cellular uptake efficiency of the drug vehicles greatly affects the therapeutic efficacies of drug release. Drug was labelled with rhodamine B (RhB) for studying the cellular uptake mechanism. Permeation of drug from the surroundings into the cell cytoplasm through cell membrane is essential to understand its consequence towards the cell. Here, drug molecules from the drug carriers are in contact with the cell and its efficacy to kill the cells mainly depends on its uptake inside the cell through cell membrane. In this work, drug is tagged with rhodamine B and embedded in D-P-L matrix. Rhodamine tagged drug penetrate through cell membrane, and can easily be delivered into cell cytoplasm which is directly correlated with efficient cell killing. For first couple of

hours, pure drug labeled with RdB could not penetrate the cell membrane, as evident from no fluorescence up to 5 h while a certain amount of drug was penetrated into the cell in 24h as shown in (***Figure 6.7a)***. In contrast, sufficient fluorescence was noticed for D-P-L-D in 1 h predominantly, it gradually entered the cell cytoplasm in a uniform, dense manner, which was clear from the fluorescence image, while meager fluorescence was observed in pure drug tagged with rhodamine.

Importantly, the cell killing efficiency towards Hela cells increases with time for drug loaded brush copolymers and reaches up to 75 % after 72 h of incubation as opposed to meagre killing of 25 % observed by pure drug in the similar time frame. In case of pure drug due to its early release it is exposed to cells immediately which results in higher killing on day 1, whereas controlled release from brush copolymer results in higher killing of cells for prolonged time interval. Here it is worthy to mention that poor availability of pure drug for prolong time (due to its early consumption) could not maintain the effective drug concentration for killing. Instead cell proliferation occurs which leads to higher cell viability for longer time period. Rate of killing is directly related with dose of the drug When compared to control where cells were grown without any treatment both the D-P-H and D-P-L showed obvious cell growth inhibition and resulted in 75 % killing of HeLa cells till day 5 (***Figure 6.7c)***. The killing is directly related to the dose of drug in vehicle and more killing at higher doses is observed. In case of D-P-H and D-P-L showed higher cytotoxicity after 72 h of incubation than free drug as there is continuous release of drug in more sustained manner entering the nuclei of cells and is effective in killing cells. Cell viabilities were further explored by visualizing the fluorescence images of Hela cells after dual staining with acridine orange and ethidium bromide of free drug, drug loaded dextrin

(Dex-d), D-P-H-d. and D-P-L-d. Cells were incubated for 24, 48 and 72 h respectively and their health was monitored. We can contemplate that acridine orange penetrates normal or early apoptotic cells and fluoresce green while ethidium dibromide enters only damaged cell membranes or late apoptotic cells emitting orange red fluorescence. Thus AO/EB staining distinguishes well between apoptotic and dead cells. Fluorescence images of native drug exhibited significant amount of apoptotic cells after 24 and 48 h of incubation. Images of cells treated with D-P-H-d and D-P-L-d displayed higher intensity of green fluorescence in nucleus and cytoplasm showing an early apoptotic indication. However both D-P-H-d and D-P-L-d showed presence of viable and apoptotic cells as well. Reduced cell viability and higher apoptosis is observed in cells treated with brush polymers, while higher viability for pure drug on day 5 is observed (***Figure 6.7d)***, corresponding with MTT assay. Similar killing efficiencies towards B16-F10 melanoma cells and almost 80 % killing were observed (***Figure 6.7e).*** As compared to free drug, brush copolymers exerted greater cytotoxic effects. Thus the efficacy of sustained release is well reflected from cellular studies and the efficacy of sustained drug release from brush copolymers is well demonstrated with a plausible mechanism. Thus, the effect of sustained release is very much prominent in cellular studies and the efficacy of the brushes as the superior delivery vehicle is demonstrated with plausible mechanism.

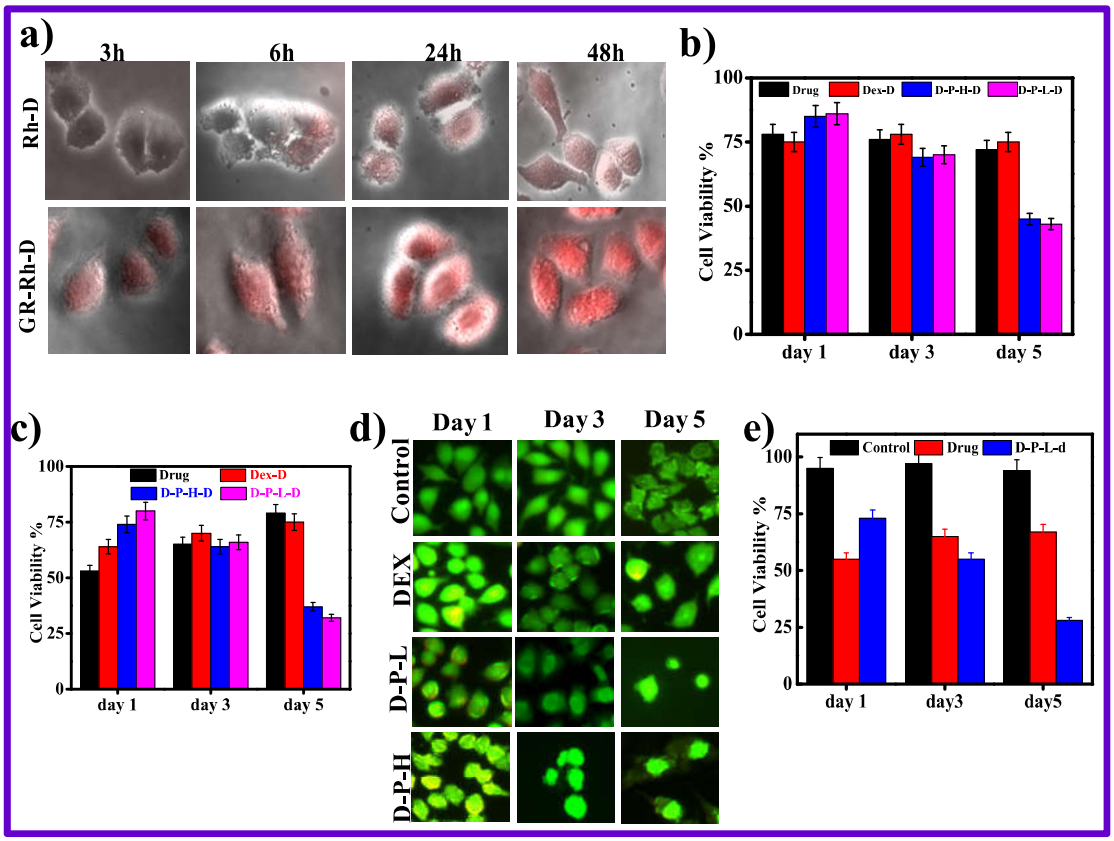

Figure 6.7: *a) Cellular uptake study into HeLa cells after different incubation time. The observed red fluorescence due to rhodamine tagged drug is observed in the Brush Copolymer with higher intensity treated at 100 μg mL^{-1}; b) Cell viability after treating with 20 μg mL^{-1} of drug; c) Cell viability of HeLa cell after treating with 200 μg mL^{-1} of drug; d)AO/EB stained fluorescence images of HeLa cells after treatment of 1,3 and 5 days respectively; e) Cell viability of B16-F10 cells after treatment with 200 μg mL^{-1}.*

6.6 In-Vivo studies on Melanoma model

Finally, the efficacy of sustained drug delivery of D-P-L-MC-D on mouse bearing melanoma tumor, induced using B16-F10 melanoma cell line, is evaluated by treating with the drug embedded D-P-L-MC over the tumor site. This gel considerably suppress the tumor growth and tumor shrank as compared to control while slight suppression of tumor is observed like the reported systems using 5-FU loaded MCL (a diblock copolymer of MPEG-b-(PCL-ran-PLLA) as an injectable hydrogel which could only inhibit the tumor

growth by 3 times of the initial tumor against 60 times increase in that of control after 18 days.[206] In another report, MPEG-PCL based diblock copolymer loaded with paclitaxel as intra tumoral drug depot inhibited tumor growth rate (mm^3/day) 20.6 against 96.4 in control (where no treatment was given).[207] In order to elude the drawback, the concept of injectable gel is applied with the understanding that the gel when placed subcutaneously will be in contact with the tumor site. Methyl cellulose is used here as it is well known for its gelling behaviour and biocompatibility[208] and can form injectable gel using appropriate concentration. D-P-L-MC-D, pure drug, and pure drug embedded in methyl cellulose gel designate as '*Gel-D*' are used for *in vivo* studies. The adavantage of this injectable gel is that it can be injected subcutaneously below the tumor site for targeted release by constant drug diffusion. The anti tumor efficacy of *D-P-L-MC-D* is investigated using B16-F10 melanoma model in albino mice and the treatment is initiated when the mice developed palpable tumor of volume approximately 20 ± 5 mm^3.

Melanoma bearing mice were randomly divided into five groups (n=5) with a subcutaneous injection of saline (Positive control), free drug(5mg/kg), drug gel(Gel-D equivalent dose of drug 5mg/kg), and D-P-L-MC-D (with same drug amount), As obvious, the tumor volume enhanced continuously with time for control (no treatment) while interestingly, the tumor volume reduced with time and a considerable shrink was observed compared to other treated groups in mice group treated with *D-P-L-MC-D* (***Figure 6.8a)***. Tumor volume in case of pure drug and drug embedded in MC gel i.e Gel-D slight tumor reduction due to faster release of drug is observed and is presented in ***Figure 6.8*****a** Quantification of relative tumor volume as a function of time is presented in ***Figure 6.8b*** clearly indicating the significant reduction in tumor size using *D-P-L-MC-D* while equivalent amount of drug

embedded in MC gel (*Gel-D*) slightly suppress the tumor growth, as compared to control. The sustained release of drug from D-P-L and D-P-L–MC achieves the therapeutic dose for longer period of time (slow and sustained release as evident from (***Figure 6.4a)*** below the tumor. While, burst release of drug from *Gel-D/pure drug* as evident from (***Figure 6.4a)*** exceeds the therapeutic dose in within short time frame thus, diffuses into the blood stream. Notably the tumor growth of free drug treated group showed initial inhibition but it also accelerated in the following days. As a result, tumor tissues do not get the required drug concentration in longer period for *Gel-D* treated mice affecting the tumor growth suppression. Furthermore the body weight ***Figure 6.8c*** of mice showed a significant loss after treatment with control (saline) and free drug as compared to D-P-L-MC-D where it remained constant, and the mean survival rate of the mice treated with D-P-L-MC-D was significantly improved compared to other groups within the experimental time of 30 days.

The design of this study is to examine whether the D-P-L-MC-D can deliver the drug in a sustained fashion by preserving the drug concentration in blood plasma within therapeutic window over extended time interval and thus can reduce the adverse side effects caused by the fast release of pure drug. As D-P-L-MC-D showed significant tumor inhibition than pure drug/gel-d,they were further evaluated for the survival time of melanoma bearing mice. The kaplan-meier survival curves are plotted and shown in ***figure 6.8d*** the survival time of D-P-L-MC-D was significantly prolonged, compared with pure drug and control. The mean survival time for control, pure polymer, pure drug, Gel-d and D-P-L-MC-D was found to be days respectively. It is worth mentioning that D-P-L-MC-D treated groups showed much higher life popagation value than pure drug which is consistent with the former results discussed above. Thus the above results indicate that D-P-L-MC-D could be

a promisisng carrier for sustained drug release and for melanoma treatment.gnificant tumor suppression within one month time without any side effect, as usually observed in conventional chemotherapy.

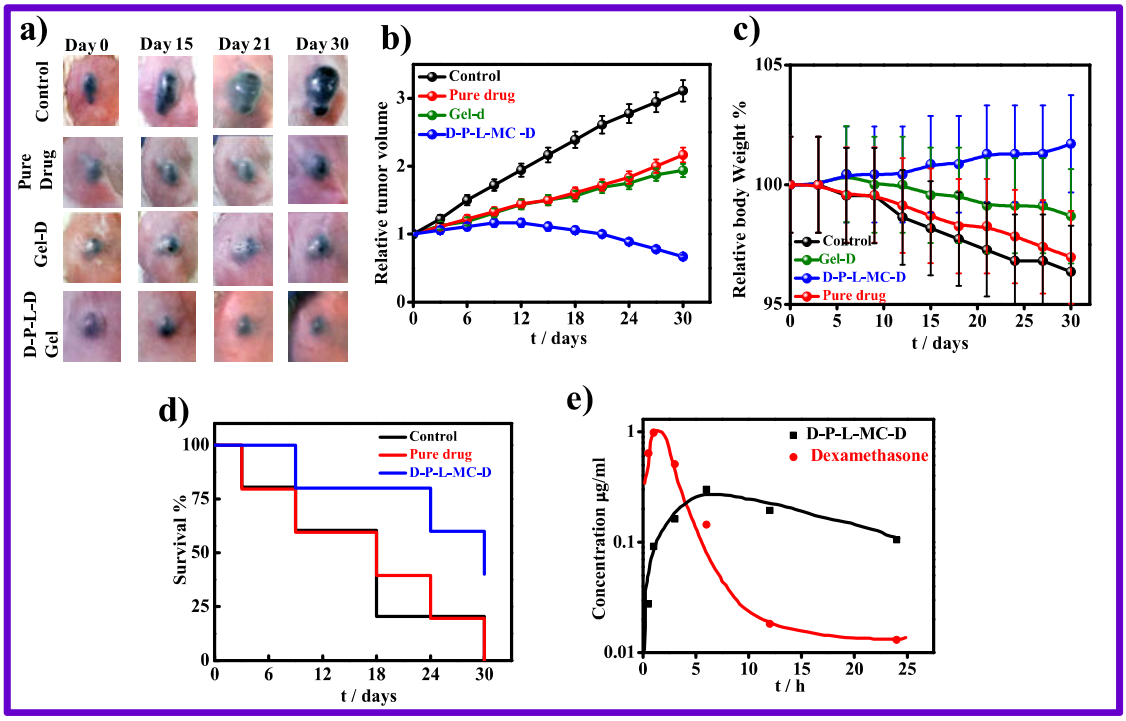

Figure 6.8*: a) Images of mice at initial day and after treatment with D-P-L-MC-D, pure drug and Gel-D indicated systems for varying time interval ; b) Relative changes in tumor volume with time treated with indicated Gels ; c) Relative changes in body weight with time treated with indicated systems; d) Kaplen Meir curve showing the survival rate of mice treated with different systems; e) Plasma drug concentration versus time profile for pure drug and D-P-L-MC-D treated albino mice after intravenous administration at 5 mg/kg body weight and an equivalent amount of drug in D-P-L-MC-D.*

To assess the *in-vivo* performance of pure drug and D-P-L-MC-D, the concentration of drug in blood stream is measured after an intravenous dose of 5 mg/kg of dexamethasone. The plasma concentration profiles of dexamethasone and D-P-L-MC-D after single intravenous administration is shown in ***Figure 6.8d***. After administration of pure drug the peak blood concentration C_{Max}=1 mg/ml appeared after 1h post dose. Nevertheless the peak

blood concentration for D-P-L-MC-D was 0.30 µg/ml and appeared after 6h of post dose, which clearly demonstrates the efficacy of sustained release from D-P-L-MC-D thereby enhancing the residential time of drug in blood stream and its slower elimination. For evaluation of toxicity imposed on vital organs histopathological analysis was carried out. Here in this work H&E staining of important organs liver, kidney, spleen and tumor tissues excised after treatment is performed for estimation of toxicity caused by pure drug and drug loaded systems. The stained images of Melanoma, treated with D-P-L-MC-D exhibited severe cell death displaying greater necrotic areas with nuclear shrinkages against higher cell density in control and D-P-L-MC treated mice, while in pure drug and gel-d treated mice slight cell damage was observed, which is derived from their cell killing efficiency presented in ***Figure 6.9a.*** These remedial effects arising from D-P-L-MC-D are due to sustained release of drug from D-P-L-MC-D maintaining the drug concentration at tumor vicinity for longer time. Hence preserving the bioavailability of drug and causing the melanoma shrinkage or a better inhibition. From liver histogram of pure drug severe damage showing inflammation in portal tract and deformation in hepatocytes shape and size was noticed, while the liver histogram of mice in *D-P-L-MC-D* treated group displays normal architecture of hepatocytes. However, no such acute toxicity is observed in the liver of mice pure polymer and control. Kidney of mice treated with *pure drug* and *Gel-d* shows slight focal tubular injury while in other groups kidney health is preserved. Spleen in all the systems displayed no damage and normal architecture was maintained.

Biochemical assay including liver and kidney function tests has been carried out to evaluate the liver/kidney dysfunctions arising from the uptake of the pure drug. Liver enzymes like alanine aminotransferase (ALT) and aspartate aminotransferase (AST) are the

critical parameters for evaluation of proper liver function. AST and ALT values in mice treated with pure drug showed a considerable increase (ALT ~ 75 U/L and AST ~ 118 U/L) from normal values after 30 days of treatment along with a significant increase in the control group, while the mice group treated with D-P-L-MC-D displayed liver activity similar to normal mice (indicated by the respective arrows) ***Figure 6.9b***, conveying healthy nature of mice whose tumors have been shrinked. Similarly, blood urea nitrogen (BUN) and creatinine levels for kidney (treated with Gel-D, D-P-L-MC-D, and Control). Urea and creatinine levels have risen in mice treated with Gel-D, while almost a normal level is observed in mice treated with D-P-L-MC-D. This is to mention that the urea and creatinine levels in the control groups are almost similar to those of the Gel-D-treated mice. As a consequence, the liver and kidney are severely affected by the administration of the pure drug, Thus pure drug/gel-d is found to damage vital organs, which is common in conventional chemotherapy for cancer treatment due to burst release of drug within very short time frame exceeding the therapeutic window, while the slow and steady release behaviour from the prepared injectable gel did not cause any adverse effect on vital organs by maintaining the concentration of drug within required regime for longer period and causing effective melanoma cell killing.

Further the immunohistochemistry of tumor tissues stained with MIA a protein specific to melanoma cells was performed. MIA is an early indicator of tumor progression relapse and metastasis.[231] targeting MIA which is expressed only on melanoma cells the adverse reaction of treatment can easily be visualized with MIA inhibitory compounds. The expression of this protein is maximum if more melanocytes are present which is clearly

revealed from immunostained tumor images of control showing huge brown area signifying MIA expression ***Figure 6.9c***.

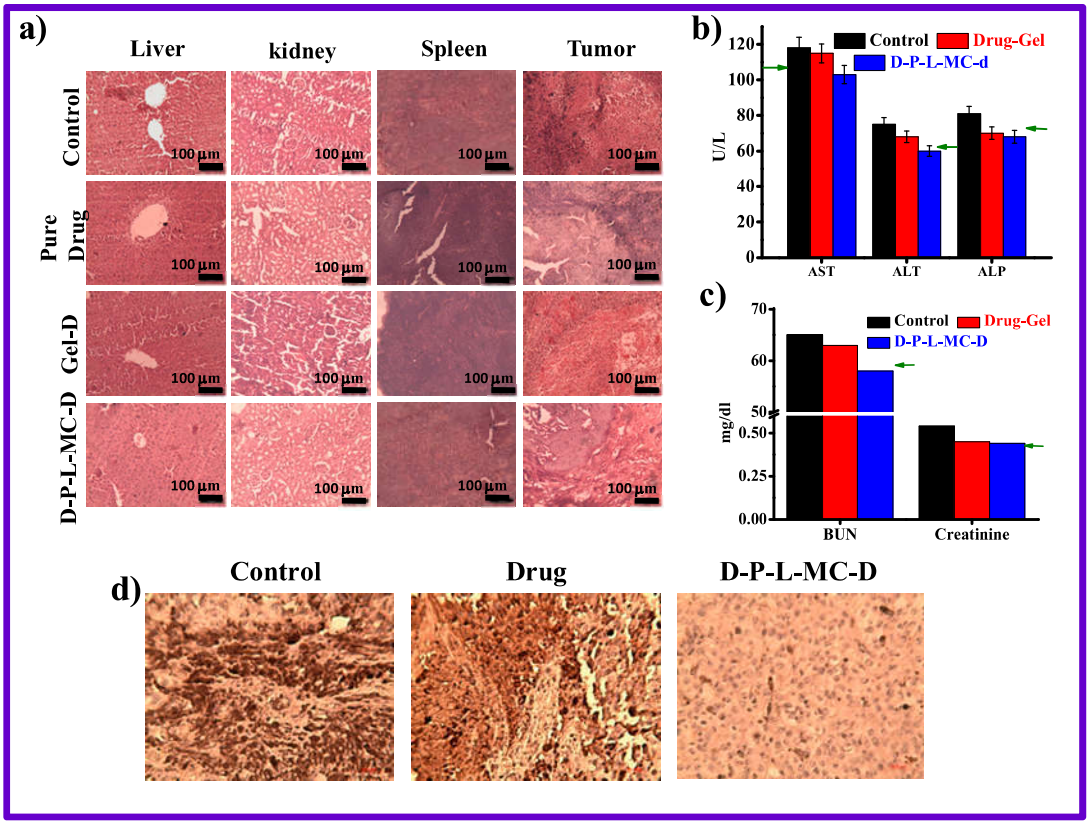

Figure 6.9: *a) Histopathological images of vital organs after treatment; b) Biochemical parameters, Hepatic function test including AST, ALT, and ALP: c) Renal function namely BUN and Creatinine of the mice treated with Gels. Corresponding values of healthy mice are indicated by the arrows; d) MIA stained tumor tissues of control, drug and D-P-L-MC-D at magnification 10X.*

Significant and homogenous MIA protein expression was detected in control and pure polymer but not in D-P-L-MC-D treated mice. Since within tumor of control MIA expression was observed in vast majority signifying huge number of melanocytes.[232] Hence, biocompatibility and efficient cell killing property of drug loaded brushes make them versatile drug delivery carrier for subcutaneous delivery of therapeutic agents particularly for tumor treatment without any side effect.

6.7 Conclusion

In conclusions, we have designed dextrin and polyurethane based different brush copolymers and its injectable gel by maintaining hydrophobic balance to regulate the release of hydrophobic anti cancerous drug (dexamethasone). The efficacy of the gel is visualized for its sustained release which follows Fickian kinetics, a diffusion controlled process. The developed brushes are biocompatible while the drug embedded brushes exhibit very high cell killing efficiency (78%) as compared to native drug in similar concentration and time. The interactions between drug and brushes are revealed from calorimetric and spectroscopic studies, along with hydrophilic hydrophobic balance of the brushes are responsible for its controlled release capability. The embedment of drug encapsulated brushes MC hydrogels makes the system as injectable gel allowing its easy placement beneath the tumor site for its efficient delivery in local area. In-vivo studies using albino mice clearly demonstrate the efficacy of significant tumor suppression within one month time without any side effect, as usually observed in conventional chemotherapy. Hence, biocompatibility and efficient cell killing property of drug loaded brushes make them versatile drug delivery carrier for subcutaneous delivery of therapeutic agents particularly for tumor treatment without any side effect.